IOPscience iopscience.iop.org

Home Search Collections Journals About Contact us My IOPscience

Study of spin-transfer-induced dynamics in spin-valves for current-perpendicular-to-plane magnetoresistive heads

This article has been downloaded from IOPscience. Please scroll down to see the full text article.

2007 J. Phys.: Condens. Matter 19 165208

(http://iopscience.iop.org/0953-8984/19/16/165208)

View the table of contents for this issue, or go to the journal homepage for more

Download details:
IP Address: 129.252.86.83
The article was downloaded on 28/05/2010 at 17:51

Please note that terms and conditions apply.

IOP PUBLISHING JOURNAL OF PHYSICS: CONDENSED MATTER

J. Phys.: Condens. Matter **19** (2007) 165208 (12pp) doi:10.1088/0953-8984/19/16/165208

Study of spin-transfer-induced dynamics in spin-valves for current-perpendicular-to-plane magnetoresistive heads

Alina Deac[1,2,4], Yue Liu[3], Olivier Redon[1,2], Sebastien Petit[1], Min Li[3], PoKang Wang[3], Jean-Pierre Nozières[1] and Bernard Dieny[1]

[1] Spintec, Commissariat à l'Energie Atomique, 17 Rue des Martyrs, 38054 Grenoble, France
[2] Commissariat à l'Energie Atomique/Direction de Recherche Technologique, 17 Rue des Martyrs, 38054 Grenoble, France
[3] Headway, 678 Hillview Drive, Milpitas, CA 95035, USA

E-mail: alina.deac@spin.mp.es.osaka-u.ac.jp

Received 30 June 2006, in final form 25 October 2006
Published 6 April 2007
Online at stacks.iop.org/JPhysCM/19/165208

Abstract

We have investigated spin-transfer effects in complex spin-valve pillars developed for current-perpendicular-to-plane (CPP) magnetoresistive heads. The structure of the samples included an exchange-biased synthetic pinned layer; both the reference and the free layer were laminated by inserting ultrathin Cu layers. Despite the low thickness of the polarizer, our results show that the free layer can be switched between the parallel (P) and the antiparallel (AP) states by applying current densities of the order of 10^7 A cm^{-2}. Due to the use of exchange-biased structures, the stability phase diagrams could be obtained in the four quadrants of the field (H)–current (I) plane, for static as well as for dynamic experiments. Microwave measurements demonstrate the existence of several spin-transfer induced precession regimes, as well as the non-equivalence of the two bias polarities, given the influence of the non-homogeneous fields in the system.

(Some figures in this article are in colour only in the electronic version)

1. Introduction

The conventional magnetoresistive heads used in computer disk drives are based on the giant magnetoresistance (GMR) of spin-valves, with the current flowing parallel to the interfaces of the spin-valve stack (the so-called 'current-in-plane geometry'). However, owing to the steady increase in the storage areal density of disk drives, this technology is nowadays close to its

[4] Present address: Graduate School of Engineering Science, Department of Materials Engineering Science, Osaka University, Toyonaka, Osaka 560-8531, Japan.

 © 2007 IOP Publishing Ltd Printed in the UK

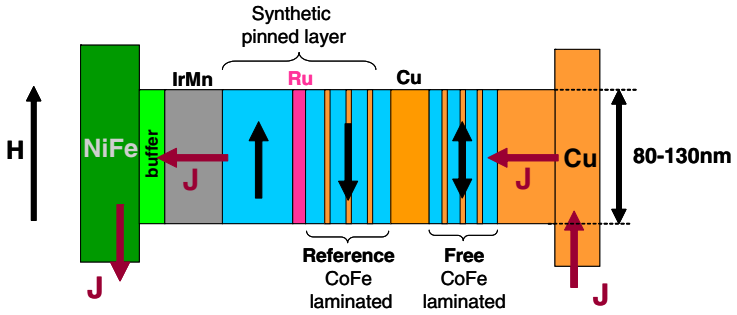

Figure 1. Sample structure and sign convention for current and field. The spin-valves were sputtered on AlTiC substrates and then patterned using a process involving electron-beam lithography and a lift-off step. The bottom current line was patterned from a NiFe layer, and was meant to constitute one of the shields of the read-head device. The top current line was made of Cu.

physical limit. New read-heads have recently been proposed and commercialized, using as sensor a magnetoresistive (MR) element in which the current is flowing perpendicular to the plane of the layers. Though the CPP geometry offers larger signal amplitude and better spatial resolution, novel unwanted phenomena are also susceptible to appear. Of particular interest are spin-transfer effects, first predicted by Slonczewski [1] and Berger [2].

Spin-transfer has been experimentally studied by various groups in pseudo-spin-valves (typically Co/Cu/Co), spin-valves and magnetic tunnel junctions, usually patterned into pillars with a lateral size of the order of 100 nm [3–14]. The current densities required to observe current-induced magnetization switching or magnetic excitations are in the range 10^6–10^8 A cm^{-2}, that is, of the same order of magnitude as the currents used in CPP-MR heads. It is therefore important to understand and master spin-transfer effects in structures designed specifically for such applications, as they may alter the functioning of the device.

2. Samples

We present here a study of spin-transfer-induced magnetization dynamics in spin-valves developed for CPP-GMR heads. The structure of the samples, shown schematically in figure 1, was the following: IrMn7/AP2 3 nm/Ru0.8/AP14.8/Cu3/F3.6/Ta (the thicknesses being given in nm). AP1 (polarizing/reference) and F (free) are CoFe layers, laminated by inserting three ultra-thin (0.3 nm) Cu layers. The purpose of the lamination is to increase the resistance of the part of the spin-valve which is active from the point of view of the CPP-GMR (AP1/Cu/F). An enhancement from 1.5% to 2.2% of the CPP-GMR was found compared to similar non-laminated multilayers [15]. AP2 was a 3 nm thick CoFe layer.

The spin-valves were subsequently processed in order to obtain pillars with square cross-section (with rounded corners) and (actual) lateral size varying between 80 and 150 nm.

The resistance of the samples ranged between 5.6 and 8.8 Ω, due to lateral size and contact resistance variations from pillar to pillar. The coercivity of the free layer (10–150 Oe) was lower than reported for previous experiments. The dispersion is probably caused by differences in the detailed shape of the pillars, especially at their edges. The magnetostatic interaction between the free and the pinned layer was relatively weak, due to the use of an almost compensated synthetic antiferromagnetic (SAF) pinned layer. The stray field on the free layer favoured the antiparallel state and was related to a dominant interaction with AP1, which was thicker than AP2 and closer to the free layer. Therefore, for low sense currents, most samples exhibited a

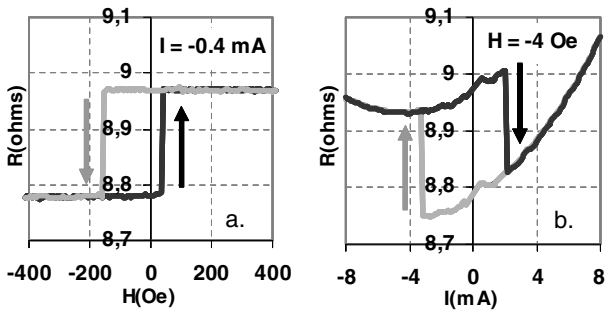

Figure 2. (a) Magnetoresistance loop corresponding to the switching of the free layer of sample 1 between the parallel (low-resistance) state and the antiparallel (high-resistance) configuration, measured with a sense current $I = -0.4$ mA. The black (grey) curve is measured for increasing (decreasing) fields. Negative fields are oriented along the magnetization of the pinned layer (favouring the P state). (b) Resistance versus current characteristics measured for the same sample with $H = -4$ Oe. The black (grey) curve is measured for increasing (decreasing) currents. For positive currents, the electrons flow from the pinned to the free layer, thus favouring the P alignment. The high- and low-resistance states are similar to those in (a).

shift of a few tens of oersteds of the hysteresis loop corresponding to the switching of the free layer, such that, in zero applied field, the pillars were in the antiparallel state.

The results presented here have been obtained at room temperature.

In our experimental setup, positive currents and fields are defined as follows.

(1) *Positive magnetic field* is oriented in the opposite direction with respect to the magnetization of the reference (AP1) layer; therefore, it favours the antiparallel (AP) state.
(2) For *positive currents*, the electrons flow from the reference to the free layer, favouring the parallel (P) alignment of the F and AP1 magnetic moments.

3. Current-induced magnetization switching

Figure 2(a) shows a minor magnetoresistance loop measured with a sense current of -0.4 mA for a 104 nm wide pillar. Given the thickness of the free layer, at such current densities ($\sim 10^6$ A cm^{-2}), no significant spin-transfer-induced effects are expected. The coercivity of this sample was $H_c = 91$ Oe. The magnetostatic stray field was $H_{ms} = 48$ Oe (favouring the AP state, as discussed above). The low-resistance state $R_{min} = 8.78\ \Omega$ corresponds to the P alignment, and the high-resistance state $R_{max} = 8.97\ \Omega$ to the AP configuration. The MR amplitude is 2.16%.

Figure 2(b) presents a resistance versus current curve measured close to zero applied field for the same sample as in figure 2(a). The switching currents are $I_c^{AP-P} = 2$ mA ($j_c^{AP-P} = 2.52 \times 10^7$ A cm^{-2}) and $I_c^{P-AP} = -3.3$ mA ($j_c^{P-AP} = -4.16 \times 10^7$ A cm^{-2}). Their polarity is in agreement with our sign convention and their order of magnitude is similar to other values so far reported in the literature. As both in the MR and in the $R(I)$ scans the transitions between the two states are very sharp, the free layer is probably switching between two uniformly magnetized states.

Figure 3 shows the evolution of the resistance versus current characteristics for different applied magnetic fields. At -51 Oe, the stray field from the SAF layer is approximately compensated, so the total field acting on the free layer is close to zero. A strong asymmetry is observed between the two switching currents, as predicted theoretically [1, 16]. Increasing

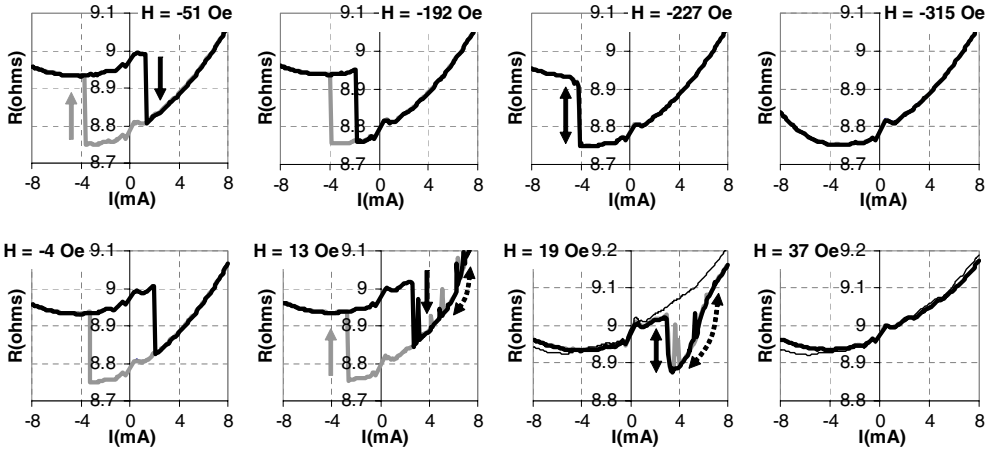

Figure 3. Resistance versus current characteristics for different values of the applied field, for sample 1. An applied field of −51 Oe approximately compensates the magnetostatic stray field from the SAF layer. The thin black line on the 19 and 37 Oe scans marks the resistance variation with the current, measured at 600 Oe, when the sample remains in (or close to) the AP state.

the external negative field induces a shift of the loop towards more negative currents. The AP–P transition moves more slowly at low fields (between 37 and −140 Oe, approximately), and more quickly at larger fields. Simultaneously, the coercivity is gradually reduced, the AP–P transition being shifted more than the P–AP one. At −227 Oe, the curve is almost reversible. At −315 Oe, the maximum applied current is no longer sufficient for inducing a P–AP transition, and the sample stays in the P state (under the influence of the applied field). This configuration (when the applied field is oriented along the magnetization of the reference layer) has been investigated by several other groups in various samples [3–14]. The general trends exhibited by our pillars are found to be consistent with previous reports.

Considerably fewer data have been published for the opposite field polarity (favouring the parallel state). For our samples, the behaviour in positive fields is rather unusual (figure 3, bottom line of graphs). Between −51 Oe (zero total field on the free layer) and 15 Oe, the loops are hysteretic and the two transitions shift towards positive current with increasing field, as expected. However, in low applied positive fields (see for example the curves measured at 13 and 19 Oe), the P state is unstable and shows evidence of random noise. The noise diminishes when increasing the field, but, at the same time, a gradual reversible transition towards a higher resistance state appears for high currents. Surprisingly, this second transition is present even at fields where the $R(I)$ loops are hysteretic (13 Oe). The onset of this transition is moving towards lower currents when the field is increased. Simultaneously, the AP → P transition induced by spin-transfer is moving towards higher values of the current. For $H > 37$ Oe, the sample remains in (or close to) the AP state and no clear switching is observed.

As a consequence of the different composition of the top and the bottom current lines (Cu and NiFe, respectively), applying a current through the pillar induces not only Joule heating, but also Peltier cooling/heating, depending on the sign of the applied bias. As such, at high fields, where no current-induced switching is observed, the resistance variation with the current is highly asymmetric. We estimate that, for sample 1, increasing the current from 0.4 to 8 mA yields a temperature increase of about 50 °C. For negative current, the temperature variation is expected to be less than 10 °C in the measured current range [17].

A current–field stability phase diagram can be reconstructed by plotting the critical lines, defined as the two switching currents as functions of the applied field as long as the curves

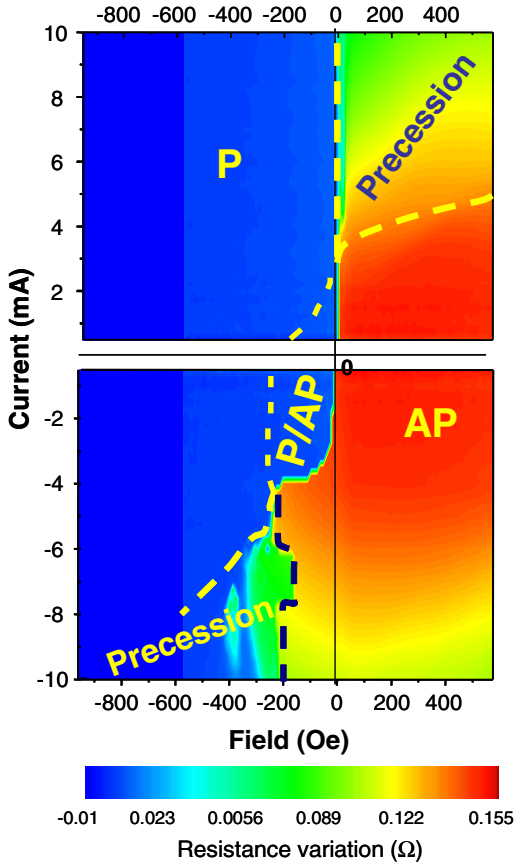

Figure 4. Static phase diagram for sample 2. The colour scale represents the resistance variation with respect to the P state resistance. The superimposed dotted lines are the critical lines which mark the switching currents at low fields, where the $R(I)$ curves are hysteretic, and the beginning and the end of the transition between the two states at fields where current-induced switching is reversible.

are hysteretic, or the beginning and the end of the current-induced transitions for fields where switching is reversible. An alternative way of plotting the static phase diagram is to represent the variation of the resistance measured at a given current and field, with respect to the resistance of the parallel state. Figure 4 presents the resistance variation versus current and field contour plot for sample 2. The superimposed dotted lines mark the critical lines obtained as described above. The results of static characterization are very reproducible from sample to sample, taking into account size variations on the wafer.

Four distinct regions can be identified in the current–field phase diagram: (1) the coercivity area, in the centre, where both the P and AP states are stable; (2) one region where only the P state is stable; (3) one region where only the AP state is stable; and (4) two areas where neither state is stable, where stable precession states are expected theoretically [18].

The general shape of the phase diagram, as well as the existence of the four types of region, can be well understood within a simple macrospin model, by analysing the stability conditions of the solution of the Landau–Lifshitz–Gilbert equation including the spin-torque term, for the P and AP states [18]. Based on this model, a detailed discussion of spin-transfer-induced switching for our samples has been presented elsewhere [17].

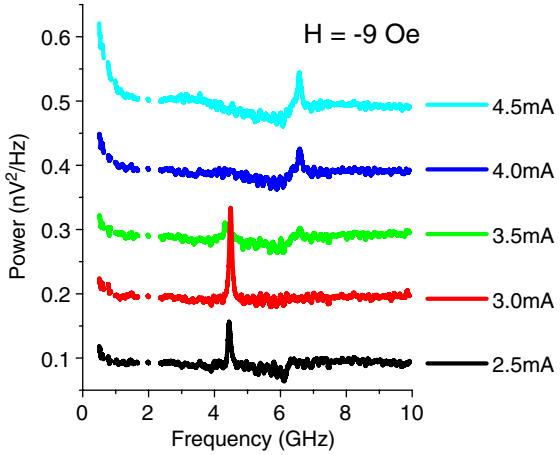

Figure 5. Microwave spectra measured for sample 2 at −9 Oe, in the small-angle FMR precession regime. The current values are as indicated on the figure. The zero-current background noise and the amplification have been subtracted. The signals are not normalized with respect to the current. (Figures 6, 7, 9 and 10 are plotted in a similar fashion.)

One feature which the macrospin model fails to explain is the presence of the gradual transition towards the AP state at positive current, in the (small) positive applied field range, as well as the random noise measured under the same conditions (as seen on the $R(I)$ curves measured at 13 and 19 Oe in figure 3). For example, for an applied field of 13 Oe, both the magnetostatic field from the pinned layer and the external field favour the AP orientation of the two layers. Starting with the sample in the AP state, when sweeping the current from negative to positive values, the spin-transfer-induced transition occurs at $I_c^{\mathrm{AP-P}} = 2.7$ mA. Since, for positive currents, the electrons flow from the pinned to the free layer, increasing the current should not change the state of the sample, according to the macrospin model. However, around 6 mA, the free layer starts to relax out of the P state. The system evolves to a resistance level which is closer to that of the antiparallel state (favoured by the field) than to that of the parallel configuration (favoured by the current). Such behaviour could solely be justified under the effect of increasing positive/inhomogeneous field, like the Oersted field. These effects are expected to be more obvious in ranges of current and field where the sample should be in the P state, which is destabilized both by the magnetostatic interaction between layers and the considerable temperature increase experienced by the sample for positive currents. Micromagnetic simulations are necessary to achieve a quantitative analysis of the matter.

4. Different precession regimes excited by the current. Static versus dynamic phase diagram

Microwave spectra were measured for both polarities of current and field using a method and an experimental setup similar to that described in [13]. In the case of sample 2, the current was varied between −10 and +10 mA with a 0.5 mA step, and the external field between −850 and +550 Oe with a 50 Oe step.

Similar to Co/Cu/Co pillars [13, 19], our complex spin-valves exhibited several precession regimes, depending on the amplitude of the applied current and field.

(1) Figure 5 shows microwave spectra measured at −9 Oe for currents up to 4.5 mA for sample 2. The first signal is resolved for $I = 2.5$ mA, that is, when the applied current

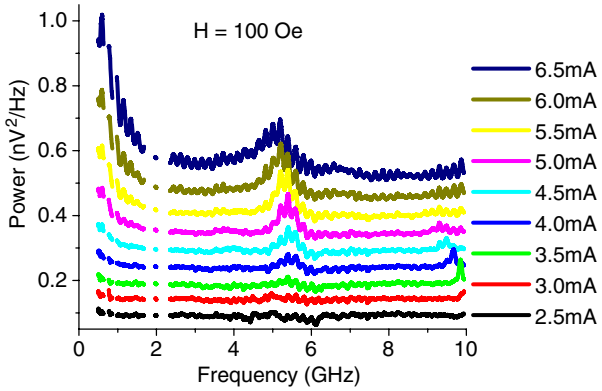

Figure 6. Microwave spectra measured for sample 2 at 100 Oe, currents between 2.5 and 6.5 mA. The current range where the signals shift to lower frequencies as the bias is increased is identified as a clam-shell precession regime. The oscillations superimposed on the signals are caused by reflections of the signal between the amplifier and the spectrum analyser.

equals $I_c^{AP\to P}$ on the -9 Oe $R(I)$ characteristics. According to reference [20], this peak corresponds to a virtually uniform precession of the magnetization of the free layer, excited by the spin-polarized current. The second harmonic, which should appear in the scanned frequency range, is predicted to be considerably lower than the fundamental and is probably covered by the noise.

The amplitude of the initial peak grows when increasing the current up to 3 mA, roughly as the square of the current, but no frequency shift is measured. Between 3 and 3.5 mA, the peak splits in two, so that the amplitude of the original 4.5 GHz signal drops considerably. The second peak appears around 6.5 GHz, and thus cannot be considered a harmonic of the first one. As the current is increased to 4.5 mA, more and more power is pumped into the second peak, and the initial signal diminishes visibly; neither of the two peaks shifts with the current.

As the signal frequency is independent on the current, but changes with the field, this low-bias mode is usually interpreted as small-angle ferromagnetic resonance (FMR) [13, 19]. Increasing the current leads to peak widening and loss of amplitude, and eventually peak splitting and mounting $1/f$ noise, which micromagnetic simulations attribute to an increasing incoherence of the local moments' precession [19, 20].

(2) At intermediate currents (5–7 mA), the peaks shift towards lower frequencies as the current is increased (red shift), as seen in figure 6. Simultaneously, the signals broaden and the second harmonic becomes visible on the spectra. This change of dynamic regime marks the onset of the second transition discussed in the previous paragraph (which appears on the $R(I)$ curves in figure 3 measured at 13 and 19 Oe). As the current is increased, the $1/f$ noise continues to rise, attaining amplitudes considerably larger than the main precession signal. Both macrospin calculations [13] and full micromagnetic simulations [19] identify this regime as large-angle, approximately in-plane precession (clam-shell precession).

(3) At even higher currents (between 7.5 and 10 mA) and low fields, the spectra are dominated by a remarkably high-power peak, centered around 0.5–2 GHz (figure 7). The highest signal is about 50 times larger than the maximum amplitude reached in the first two regimes. This feature (which cannot be interpreted based on a simple macrospin model [13]) is explained by micromagnetic simulations [19] as resulting from chaotic jumps of the magnetic moments between two stable precession orbits: one given by the

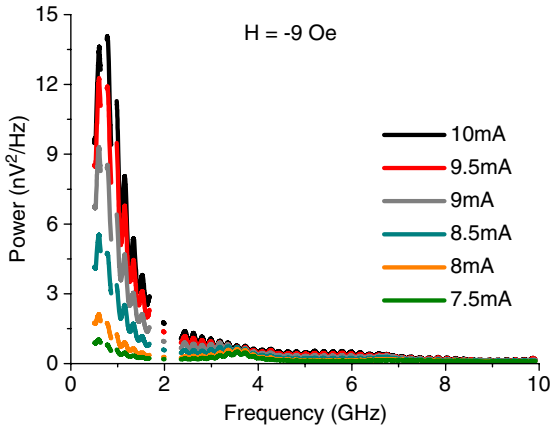

Figure 7. Microwave spectra measured for sample 2 at −9 Oe, in the high-frequency telegraph noise regime. The spectra are dominated by the high-amplitude, low-frequency peak, attributed to chaotic jumps of the magnetic moments between a precession orbit given by the field, and a second trajectory, given by the current. The amplitude of the peak is related to the resistance variation between the two orbits.

current and a second one given by the field. This is the so-called high-frequency telegraph noise regime.

When the current is held constant and the field is increased, the maximum power reached by the low-frequency peak is diminished (not shown; see the phase diagram: figure 8). The absolute maximum power measured for sample 2 was attained at −9 Oe and 10 mA. Similarly, in the small-angle FMR and the clam-shell precession regimes, the $1/f$ noise is decreasing with the field, since higher fields tend to render the dynamics of the local moments less chaotic [19].

A dynamic phase diagram can be defined by plotting the power integrated on the measured frequency range for a fixed current and field, normalized to the square of the applied current, since the output power is expected to vary as I^2. In the case of Co/Cu/Co pillars under the effect of a field (current) favouring the P (AP) state, it has been shown that the static and dynamic phase diagrams can be well compared [13].

Figure 8 presents the dynamic phase diagram of sample 2, plotted as described above. As expected, a good agreement was found between the static and dynamic phase diagrams. Generally, large normalized integrated power is obtained in the regions where the static resistance has an intermediate value between those of the parallel and antiparallel configurations. In both quadrants of the phase diagram, the highest level of normalized integrated power is reached for the maximum applied current (±10 mA), for values of the field which mark the exit from the coercivity region in static measurements. In the areas where relatively coherent small-angle precession states are excited, the resistance is found (unsurprisingly) to be very close to that of the corresponding state (P or AP).

5. Influence of the bias polarity on the precession stated excited by the spin-polarized current

As was the case for static measurements, microwave spectra obtained for negative currents and fields (current/field configuration investigated in previous studies) showed similar trends to those evidenced by simple Co/Cu/Co nanopillars [13]. High-frequency experiments for

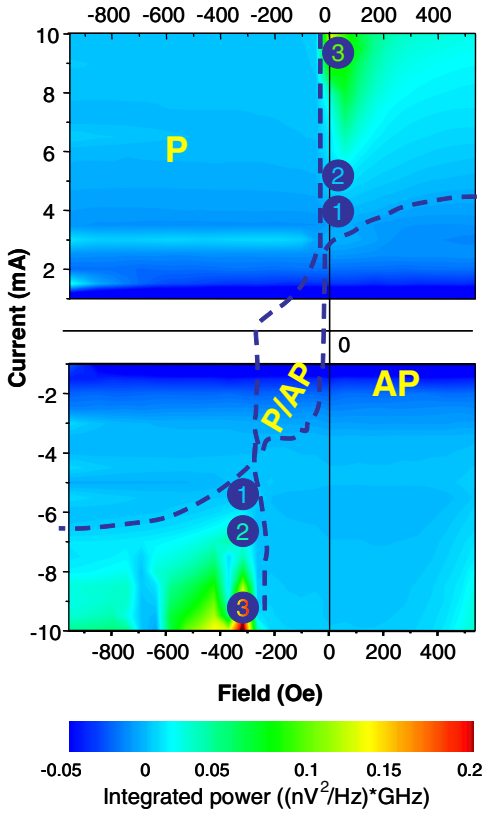

Figure 8. Dynamic phase diagram for sample 2, obtained by measuring microwave spectra for each value of current and field and plotting the corresponding integrated power, normalized by the square of the current. The colour scale corresponds to the amplitude of the normalized integrated power. 1, 2 and 3 mark the three precession regimes described in the text. The superimposed dotted lines are the critical lines determined from static measurements.

currents and fields of the opposite sign indicated that the two current polarities are not equivalent.

For sample 2, the first signals are resolved for 2.5 and −6 mA, respectively. As mentioned in the previous paragraph, the frequency of the peaks is independent of the applied current and they are attributed to small-angle FMR precession. Figure 9 shows the field dependence of the small-angle FMR frequency, for positive and negative bias. At 2.5 mA, the signals attain a maximum amplitude of 0.15 $nV^2\ Hz^{-1}$, while less than 0.1 $nV^2\ Hz^{-1}$ is the best value obtained for negative bias. We point out these values have not been normalized with respect to the applied current. Moreover, the peaks are usually broader in negative current and the $1/f$ tail is more important (not shown), suggesting that the dynamics is very likely less coherent for negative than for positive bias [19].

The dashed lines in figure 9 mark the FMR frequencies calculated with Kittel's formula [21], and assuming $4\pi Ms = 16\,000$ Oe (the same value as considered for fitting the static phase diagram [17]). The actual anisotropy is unknown, but can be evaluated from the measured room-temperature coercivity (supposing the volume of the free layer is known) [22]. For sample 2, considering a lateral size of about 100 nm and the experimentally determined $H_c = 100$ Oe, the anisotropy is estimated to be around 180 Oe. The FMR frequencies

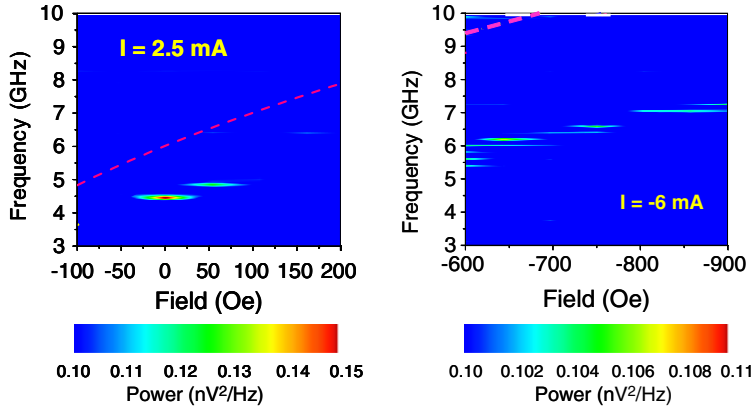

Figure 9. Dependence of the small-angle FMR frequency on the applied field, in positive (left) and negative (right) bias. 2.5 and −6 mA are the lowest currents where microwave signals are resolved. The dotted pink lines are fits using Kittel's formula and $4\pi Ms = 16\,000$ Oe and $H_k = 180$ Oe.

calculated with these parameters are about 1 GHz higher than the values measured for positive currents. The agreement is considerably worse for negative currents, where the predicted frequencies are about 50% larger than obtained experimentally. A similar disagreement was previously obtained for Co/Cu/Co pillars in the same current/field configuration [13] (field applied along the magnetization of the reference layer and current favouring the AP state), and was quantitatively explained by correctly taking into account the incoherency of the dynamics of the local moments [19]. A similar interpretation would lead to the conclusion that in our pillars precession is more coherent for positive current, as inferred from peak amplitude and width, and $1/f$ power considerations as well (as mentioned above).

Though a quantitative analysis would require full micromagnetic simulation, it is possible to suggest an interpretation for the influence of the bias sign on spin-transfer-induced dynamics, based on previous micromagnetic studies and static experimental results.

Two likely sources of increased incoherency in negative bias can be identified: the stray field from the SAF layer and the Oersted field. The negative field opposes the dipolar interaction from the reference layer, which is highly inhomogeneous (strong at the edges and weak in the centre of the layer). At rather low applied fields, such as considered here, it is possible that the total field acting on the local moments at the edges of the cell has an opposite polarity compared with the centre of the pillar, so the dynamics is expected to be more chaotic. Moreover, static experiments have already demonstrated that spin-transfer is more efficient for positive than for negative currents. Indeed, it takes about twice as much negative current to produce the same effect (switching, for example) as a given positive current. Evidence of small-angle precession is obtained for 2.5 and −6 mA, respectively. Though the spin-torque amplitude should be roughly the same, the Oersted field, which is proportional to the current and a source of incoherence because of its spatial non-uniformity, is obviously higher at −6 than at 2.5 mA.

In the high-frequency telegraph noise regime, experiments showed that about twice as much power is reached in negative currents, as compared with the opposite bias polarity (figure 10). As explained in the previous paragraph, the 1 GHz peak is attributed to chaotic jumps of the magnetic moments between two precession trajectories, one given by the field and one given by the current. The signal amplitude is related to the resistance variation between the two orbits.

For negative currents and fields, the current gives a precession trajectory in the vicinity of the AP state (which is always stable in current, as demonstrated by static experiments),

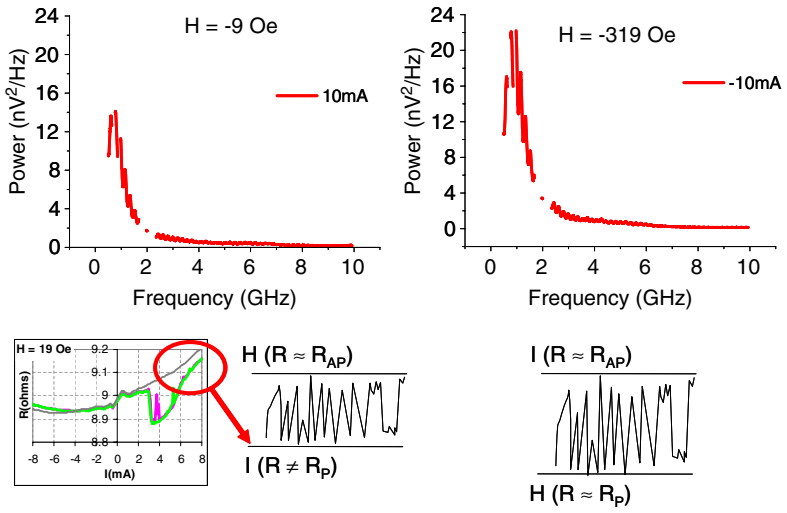

Figure 10. Top: the telegraph noise peak in negative current (−10 mA) reaches almost twice the amplitude attained for similar positive currents (10 mA). Bottom: resistance versus current curve measured for sample 1, showing the second transition towards an intermediate resistance level in high positive currents. Schematic drawing of high-frequency telegraph noise for the two configurations, with the corresponding resistance variation.

while the field favours an orbit close to the P state (which is stable in field), so almost the full GMR variation can be reached. In the opposite current/field configuration, the field determines a precession trajectory close to the AP state (stable in field), while the current brings the free layer into an intermediate resistance (dynamic) configuration (see the second transition in positive current on the $R(I)$ curves). The resistance variation between the two dynamic states is thus lower and the maximum amplitude reached by the 1 GHz peak will be lower than for negative currents. The static resistance measured on the $R(I)$ curves at 10 mA is probably the weighted mean (taking into account dwell times) of the corresponding resistance levels of the two dynamic states.

6. Conclusion

In conclusion, we have demonstrated that spin-transfer effects do take place in complex spin-valves developed for CPP-GMR heads. We have measured the four-quadrant I–H phase diagram both for static and for dynamic experiments. We found that in the 'coherent' regimes, namely small-angle FMR and large-angle, approximately in-plane precession, the dynamics is considerably more coherent for fields (currents) favouring the antiparallel (parallel) state. In the chaotic dynamics region, the signal corresponding to high-frequency telegraph noise is found to reach amplitudes almost twice as high for negative as for positive currents of the same intensity. Such effects are especially important in CPP-GMR heads, where the current polarity is predefined. This information may also prove interesting for potential applications towards new magnetic resonators or microwave sources for wireless telecom devices.

Acknowledgments

The authors would like to thank Professor A Vedyaev and Dr N Strelkov for fruitful discussions, and Dr U Ebels, Dr C Thirion and Dr D Stanescu for helping with the experimental setup. This

work was partially supported by the IST project NEXT (IST-37334) and the RMNT project MAGMEM II.

References

[1] Slonczewski J 1996 *J. Magn. Magn. Mater.* **159** L1
Slonczewski J 1999 *J. Magn. Magn. Mater.* **195** L261
[2] Berger L 1996 *Phys. Rev.* B **54** 9353
Berger L 1999 *Phys. Rev.* B **59** 11465
[3] Katine A, Albert F J, Buhrman R A, Myers E B and Ralph D C 2000 *Phys. Rev. Lett.* **84** 3149
[4] Grollier J, Cros V, Hamzic A, George J M, Jaffres H, Fert A, Faini G, Ben Youssef J and Legall H 2001 *Appl. Phys. Lett.* **78** 3663
[5] Urazhdin S, Kurt H, Pratt W P Jr and Bass J 2003 *Appl. Phys. Lett.* **83** 114
[6] Myers E B, Albert F J, Sankey J K, Bonet E, Buhrman R A and Ralph D C 2002 *Phys. Rev. Lett.* **89** 196801
[7] Emley N C, Albert F J, Ryan E M, Krivorotov I N, Ralph D C and Buhrman R A 2004 *Appl. Phys. Lett.* **84** 4257
[8] Sun J Z, Monsma D J, Rooks M J and Rooks R H 2002 *Appl. Phys. Lett.* **81** 2202
[9] Ozyilmaz B, Kent A D, Monsma D, Sun J Z, Rooks M J and Koch R H 2003 *Phys. Rev. Lett.* **91** 067203
[10] Covington M, Rebei A, Parker G J and Seigler M A 2004 *Appl. Phys. Lett.* **84** 3103
[11] Huai Y, Albert F, Nguyen P, Pakala M and Valet T 2004 *Appl. Phys. Lett.* **84** 3118
[12] Kubota H, Fukushima A, Ootani Y, Yuasa S, Ando K, Maehara H, Tsunekawa K, Djayaprawira D D, Watanabe N and Suzuki Y 2005 *Japan. J. Appl. Phys.* **40** L1237
[13] Kiselev S I, Sankey J C, Krivorotov I N, Emley N C, Schoelkopf R J, Buhrman R A and Ralph D C 2003 *Nature* **425** 380
[14] Covington M, Al Haj Darwish M, Ding Y, Gokemeijer N J and Seigler M A 2004 *Phys. Rev.* B **69** 184406
[15] Li M, Liao S, Chen C P, Ju K, Delille F, Strelkov N and Dieny B 2004 unpublished
[16] Stiles M D and Zangwill A 2002 *J. Appl. Phys.* **91** 6812
[17] Deac A, Lee K J, Liu Y, Redon O, Li M, Wang P, Nozières J P and Dieny B 2006 *Phys. Rev.* B **73** 064414
[18] Grollier J, Cros V, Jaffres H, Hamzic A, George J M, Faini G, Ben Youssef J, Le Gall H and Fert A 2003 *Phys. Rev.* B **67** 174402
[19] Lee K J, Deac A, Redon O, Nozières J P and Dieny B 2004 *Nat. Mater.* **3** 877
[20] Zhu J-G and Zhu X 2004 *IEEE Trans. Magn.* **40** 182
[21] Kittel C 1996 *Introduction to Solid State Physics* 7th edn (New York: Wiley) p 566
[22] Sharrock M P 1990 *IEEE Trans. Magn.* **26** 193